Chemical Physics Letters 657 (2016) 53–59

Contents lists available at ScienceDirect

Chemical Physics Letters

journal homepage: www.elsevier.com/locate/cplett

Research paper

Determination of relative positions and localizations of paramagnetic probe molecules in liquid crystal by analysis of concentration broadening of EPR spectra

Daria A. Pomogailo *, Nikita A. Paramonov, Natalia A. Chumakova, Andrey Kh. Vorobiev

The Laboratory of Chemical Kinetics, Department of Chemistry, M.V. Lomonosov Moscow State University, Leninskie Gory 1-3, Moscow 119991, Russian Federation

ARTICLE INFO

Article history:
Received 29 March 2016
Revised 19 May 2016
In final form 24 May 2016
Available online 25 May 2016

Keywords:
Concentration broadening
Nitroxide radicals
Spin probes
Liquid crystals
Magnetic dipolar interactions
Spin exchange
Molecular arrangement
EPR spectroscopy

ABSTRACT

The angular dependences of concentration broadening of EPR spectra for nitroxide spin probes in liquid crystals were experimentally measured. The obvious angular dependence of the broadening found for oriented smectic liquid crystal HOPDOB proves the paired localization of the probe molecules. The numerical calculation of the angular dependence taking into account the magnetic dipolar and spin exchange interactions have been used for quantitative determination of position of probes in the pairs. The probable localization of the probes in the smectic layer is discussed.

1. Introduction

In recent years, technological interest has been drawn to materials formed by liquid crystals with low-molecular-weight or polymer components dissolved [1–9]. Therefore, the methods useful for determination of molecular structure of such materials become important. At present, unfortunately, the experimental means for studying of the molecular structure of liquid crystals are very limited. There are few papers describing the NMR determination of orientation and translation molecular order of liquid crystalline media [10–12]. In particular, authors of [11,12] have determined the localization of admixture molecules within the smectic liquid crystalline layers.

Dipole–dipole and exchange magnetic interactions of paramagnetic particles are known to determine line shape of magnetic resonance spectra [13–18]. This circumstance is used as a source of information about the structure of solids containing paramagnetic centers. In particular, the angular dependences of EPR spectra were recorded for characterization of low-dimensional crystalline magnetics [19,20]. Earlier [21] we have demonstrated the using of EPR measurements for quantitative characterization of positions and orientation of molecules in paramagnetic liquid crystals. The method is based on the analysis of angular dependence of concentration broadening of EPR spectra. In the presented work, we develop this approach for determination of relative positions of paramagnetic probe molecules in diamagnetic liquid crystalline media. The liquid crystals 4-n-octyl-4′-cyanobiphenyl (8CB) and p-hexyloxyphenyl ester of p-decyloxybenzoic acid (HOPDOB) have been chosen as smectic materials. The structure of paramagnetic probes used are presented in Fig. 1. To acquire the angular dependence of the broadening, the EPR spectra of oriented liquid crystalline samples with different concentration of paramagnetic probes were recorded at different directions of sample axis relative to the magnetic field of the spectrometer.

2. Experimental

2.1. Materials

4-n-octyl-4′-cyanobiphenyl (8CB) (Aldrich) was used without additional purification. P-hexyloxyphenyl ester of p-decyloxybenzoic acid (HOPDOB) was synthesized in RIAP (Kiev factory of chemical agents, indicators and analytical specimens) and purified by recrystallization from ethyl acetate. The liquid crystals have nematic and smectic mesophases in the following temperature ranges (T, K):

* Corresponding author.
E-mail address: texafirin@ya.ru (D.A. Pomogailo).

http://dx.doi.org/10.1016/j.cplett.2016.05.051
0009-2614/

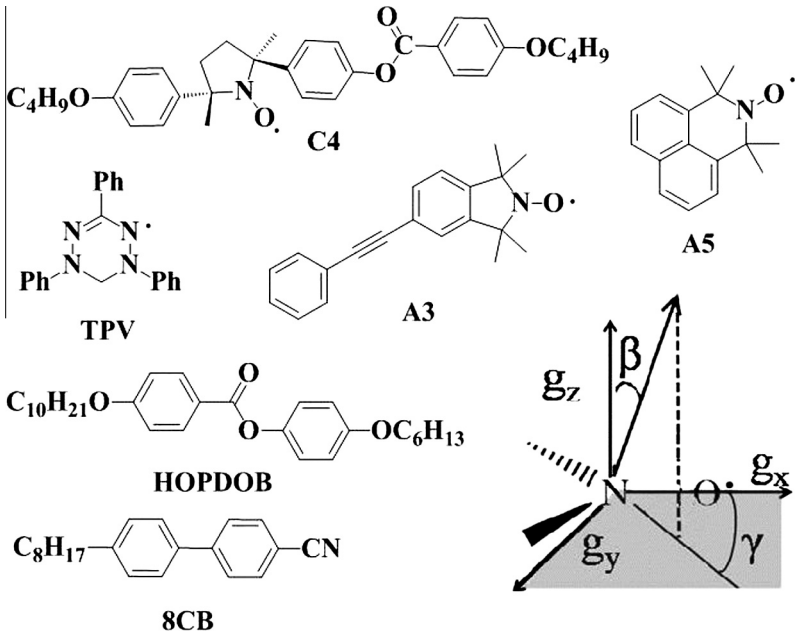

Fig. 1. Paramagnetic probes and liquid crystals used in present work; the direction of main orientation axis in molecular coordinate frame (g_x, g_y, g_z) of the nitroxide moiety is shown.

8CB: Cr-(294.2)-SmA-(305.7)-N-(313.2)-Iso [22];
HOPDOB: Cr-(335.6)-(SmE, SmB)-(317.6)-SmC-(350.6)-SmA-(356.4)-N-(362.0)-Iso [23,24].

Fig. 1 shows chemical structures of liquid crystals and spin probes employed in this work. The probe C4 was synthesized in accordance with method described in [25,26] and kindly granted by Prof. Rui Tamura (Kyoto University, Japan). The stable radicals A5 and A3 were synthesized by methods [27] and [28], accordingly, and kindly granted by Prof. Steven Bottle (Queensland University, Australia). Stable radical triphenylverdazyl (TPV) kindly granted by V.K. Cherkasov (Razuvaev Institute of Organometallic Chemistry of RAS, Nizhny Novgorod, Russia).

2.2. Sample preparation

The solutions of spin probes in liquid crystals were obtained by mixing the appropriate amounts of components and keeping the samples at temperatures of isotropic phase of liquid crystals for two hours. The 0.1 ml of solutions of spin probes with different concentrations were placed in quartz ampoules (inner diameter 3 mm) and were degassed at pressure of 10^{-3} Torr for several hours at the temperature of isotropic state of the material. The low concentration samples where changes in the EPR spectrum do not occur at further dilution were used as a reference. The samples where measurable broadening of the spectrum had been observed were used as high concentration samples. The concentration range in our experiments was $2{\cdot}10^{-4}$–$4{\cdot}10^{-2}$ M ($5{\cdot}10^{-3}$–1.0 mol%). All samples were aligned by magnetic field of EPR spectrometer (0.5–0.6 T) in the course of slow cooling of the sample from the isotropic to the mesophase state. The orientation axis of liquid crystals after the aligning was directed perpendicular to the axis of the ampoule.

2.3. Angular dependence acquisition

X-band EPR spectra were recorded with spectrometers "Varian E3" (Palo Alto, CA, USA) and "Bruker EMXplus" (Bruker Biospin, Karlsruhe, Germany). For recording of the spectrum at the mesophase temperature, the ampoule was placed into an EPR Dewar tube with airflow of required temperature. The temperature was controlled with the accuracy of ±0.5 °C. It was found experimentally that it takes 3 min for the sample temperature to equilibrate with the temperature of the flow.

A series of EPR spectra (18 or 19 in total) were recorded by rotating the sample tube relative to the magnetic field of the spectrometer. The angle χ between the sample orientation axis and the magnetic field direction was varied from 0° to 90° and from 95° to 175° with the 10° step. Below, the set of such spectra is referred to as the 'angular dependence of EPR spectra'. Angular dependences for samples with different concentration of probe A5 in liquid crystal HOPDOB are presented in Fig. 2 as typical examples. The angular dependences of spectra for other studied systems are presented in the Supplementary Material.

Angular dependences of EPR spectra at low concentrations of spin probe were used for determination of orientation of probe molecules in the aligned liquid crystals. The values of concentration broadening were determined from angular dependences of spectra at higher concentration.

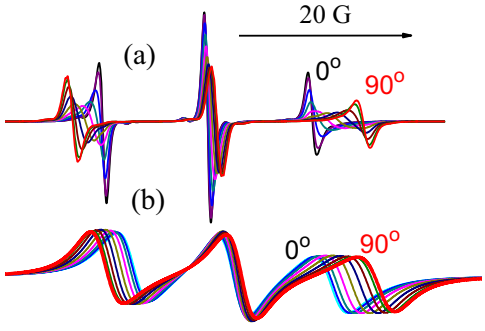

Fig. 2. Angular dependence of EPR spectra for spin probe A5 in SmC HOPDOB (352 K), concentration $2.87{\cdot}10^{-4}$ M (a) and $3.35{\cdot}10^{-2}$ M (b) The spectra recorded at 0–90° with the step of 10° are presented.

2.4. Determination of the broadening of EPR spectra

Linewidth of the EPR spectra at low concentration of paramagnetic probe is defined by magnetic anisotropy of the probe (anisotropy of g- and hfi-tensors), as well as by orientational order of aligned medium and frequency of molecular rotational motions. EPR spectra of samples with higher concentration of probe are additionally broadened by magnetic dipole–dipole and spin exchange interactions of paramagnetic particles. The concentration broadening can be measured as the difference between line widths of spectra for samples with high and low concentration of the probe [29,30]. It is well-known that anisotropy of nuclear hyperfine interaction shows itself heavily in linewidth of the outermost components of EPR spectra. The width of the central component of the spectrum, on the contrary, is least sensitive to magnetic anisotropy of probe. Therefore, the values of concentration broadening are determined from the width of the central spectral component most precisely. Two procedures were used in the present work for the measurement of linewidth. The first one is the direct measurement of peak-to-peak distance ΔHpp (fields distance between minimum and maximum points for the component recorded as first derivative curve). The second procedure is based on the numerical simulation of experimental spectral components using the convolution of Gaussian and Lorentzian functions (Voigt profile). The Fourier transform of the spectrum line was calculated as follows:

$$SF(w, \Delta H_L, \Delta H_G) = GaussF(w, \Delta H_L) \cdot LorF(w, \Delta H_G) \quad (1)$$

where *GaussF* and *LorF* denote Fourier transform of Gaussian and Lorentzian functions accordingly. ΔH_G and ΔH_L are the peak-to-peak width for Gaussian and Lorentzian components.

The Voigtian line shape can be described by different methods (see, for example, [31–34]). We have used the formulation described in [35]. The Gaussian and Lorentzian width ΔH_L and ΔH_G are determined by nonlinear least-squares fitting for every spectrum of angular dependence independently. The experimentally observed line width ΔHpp was calculated in this case using the following expression [36,37]:

$$\left(\frac{\Delta H_G}{\Delta Hpp}\right)^2 + \frac{\Delta H_L}{\Delta Hpp} = 1 \quad (2)$$

The search of the best fitting parameters was performed using the minimizing program NL2SOL [38]. The values of uncertainty calculated by this program are presented below as experimental errors of determination. The best-fit line shape coincided with the experimental one within the noise of spectra recording. The values of line width determined by the two procedures described above were practically the same.

3. Results and discussion

The angular dependences of EPR spectra for low concentration of spin probes were numerically simulated using the stochastic Liouville equation, as described in [39]. Discussion of detailed results of spectra simulation is out of the scope of the present work. It is only important here that in the course of this simulation the direction of main orientation axis in molecular coordinate frame is determined with high accuracy. This molecular orientation axis defines the predominant orientation of probe molecule relative to director of the ordered liquid crystalline medium. The examples of determination of molecular orientation axis from angular dependence of spectrum are presented elsewhere [35,39–44]. The values of angles defining the orientation of probe molecules C4, A3 and A5 in the studied media are collected in Table 1. The characteristics of molecular orientation determined earlier [43] for similar samples in the supercooled state (77 K) are presented in Table 1 for comparison. Good agreement between the molecular orientation axes determined at different temperatures can be seen.

Table 1
The angles (see Fig. 1) defining the main molecular orientation axis in the molecular magnetic reference frame.

System	β,° (mesophase)	γ,° (mesophase)	β,° (77 K) [43]	γ,° (77 K) [43]
C4-8CB	39.6 ± 0.9	90.0 ± 1.0	33.8 ± 0.7	87.8 ± 1.8
A5-HOPDOB	90.3 ± 0.3	90.4 ± 0.3	89.8 ± 5.8[a]	98.5 ± (1–2)[a]
A3-HOPDOB	115 ± 5.0	−41.5 ± 0.5	89.9 ± (1–2)[a]	−39.2 ± (1–2)[a]

[a] The data for samples of A3 and A5 in 8CB are presented, as the solubility of these probes in HOPDOB at low temperature does not allow obtaining resolved EPR spectra.

The concentration broadening of EPR spectra for samples of probe A5 in HOPDOB is illustrated in Fig. 2. Fig. 3 demonstrates the angular dependence of width of the central component for samples C4 in 8CB and A5 in HOPDOB with different concentrations. One can see in Fig. 3a that angular dependence of linewidth of C4 probe at higher concentrations is merely shifted to higher values, keeping the overall shape of the dependence. The angular dependence of concentration broadening in this system is small and comparable with experimental uncertainty. It is known that spin exchange broadening is independent of the direction of the external magnetic field. The dipole–dipole interaction, on the contrary, is essentially angular dependent. The angular dependence of dipole–dipole interaction vanishes only when paramagnetic species are randomly distributed in the sample. Thus, the probe C4 in 8CB demonstrates the spin exchange broadening, which is the result of diffusion collisions of probe molecules. The possible dipole–dipole interaction is almost isotropic and therefore it is averaged over random spatial distribution of the probe. The same results were obtained for triphenylverdazyl (TVP) radical in 8CB.

The evident angular dependences of concentration broadening of EPR spectra in our experiments were found for probes A5 and A3 in smectic HOPDOB. It is illustrated in Fig. 3b for the case of A5 in SmC HOPDOB. The dependences for A3 in HOPDOB are presented in the Supplementary Material.

For the determination of arrangement of probe molecules in the liquid crystalline structure, the theoretical simulations of the obtained angular dependences were used in the present work. The simulations were performed numerically using the procedure described in detail earlier [21]. The procedure consists in calculating the Fourier transform for the broadened component of EPR spectrum in accordance with the following expression:

$$SF(w, \chi) = \frac{1}{2\pi} \int GausF(w) \cdot LorF(w) \cdot HddF(w, \chi) d\varphi \quad (3)$$

where χ is the angle between the director of liquid crystalline medium and the magnetic field of the spectrometer; *GaussF* and *LorF* denote the Fourier transforms of Gaussian and Lorentzian functions with the width defined by spin exchange; *HddF* describes the dipole–dipole broadening for pair of molecules by following equations:

$$\begin{aligned} HddF(w, \chi) &= \cos\left(w \tfrac{Hdd}{2}\right); \\ Hdd &= \mu \tfrac{3\cos[H \cdot r(\psi, \varphi, \sigma, \alpha_L)]^2 - 1}{|r(\psi, \varphi, \sigma, \alpha_L)|^3} \end{aligned} \quad (4)$$

Expressions (4) were derived for the pair of paramagnetic centers, which are connected by the radius vector $r(\psi, \varphi, \sigma, \alpha_L)$ and are coupled by dipolar interaction [21]. The radius vector is a function of structural parameters of the ordered medium. The angle σ is the

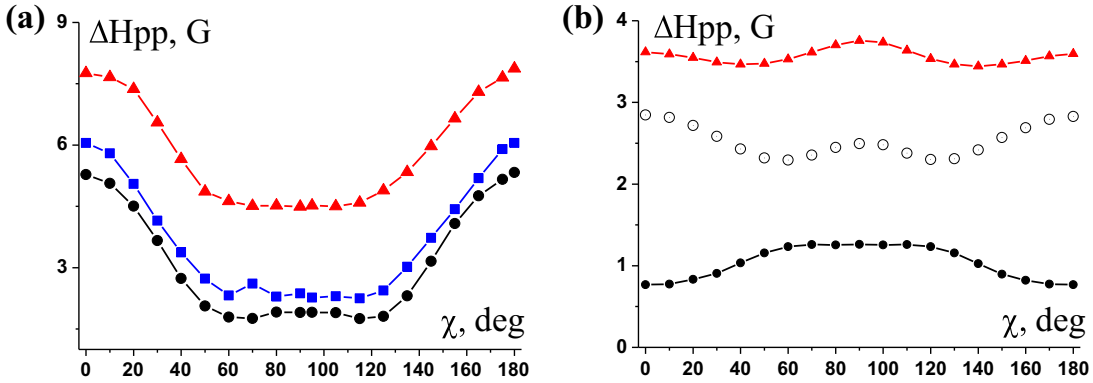

Fig. 3. Experimental angular dependences of width for central component of EPR spectrum; (a) C4 probe in smectic 8CB (304 K) at concentrations $8.37{\cdot}10^{-4}$ M (points), $2.37{\cdot}10^{-2}$ M (squares), 0.17 M (triangles); (b) A5 probe in SmC HOPDOB (342 K) at concentrations $2.87{\cdot}10^{-4}$ M (points), $3.35{\cdot}10^{-2}$ M (triangles); circles show the angular dependence of the concentration broadening (difference of width).

angle between the radius vector and the plane of the smectic layer, the angle φ is the azimuthal angle of the radius vector. The angle α_L is the tilt angle of molecular axis of the liquid crystalline molecules relative to the smectic layer normal. The angle ψ describes the macroscopic orientation of biaxial smectic layers relative to the sample. Use of all these angles is necessary for the description of the smectic C phase only. The angles α_L and ψ are equal to zero for the smectic A phase. Moreover, the expressions (4) in our experiments were found to be independent of the value of ψ, because the radius vector r was directed predominantly along the liquid crystal director (σ is close to 90°).

If the sample comprises some differently oriented layers or different interacting pairs of probe molecules, corresponding summation or integration over all possible orientations should be performed in Eq. (3). The integration over all possible values of angle φ was used in our calculations. The inverse Fourier transform of Eq. (3) produces the shape of the broadened spectrum component. The difference between the width of the broadened component and width of unbroadened component is the calculated value of concentration broadening which is angular dependent.

The concentration broadening in the considered systems is determined both by spin exchange, which is proportional to collision frequency, and by magnetic dipole–dipole interaction of pairs of probe molecules, fixed on defined distances. The exchange broadening was assumed to be the same for all probe molecules. Thus, every experimental EPR spectrum was described as a sum of exchange-broadened spectrum with fraction $(1-\alpha)$ and spectrum, broadened by exchange and dipolar interactions, with fraction α. The value of fraction α was one of the variable parameters of model. The shape of the broadened component was theoretically calculated using the following sequence of steps:

(1) The central component of experimental spectra at low concentration of the probe was simulated with a Voigt profile. The unbroadened Gaussian and Lorentzian widths, ΔH_G^0 and ΔH_L^0, were determined from this simulation.
(2) The shape of exchange-broadened component was calculated using expression (1) with the linewidth calculated as follows:

$$\begin{aligned} \Delta H_G &= \Delta H_G^0 + \Delta H_G^{ex} \\ \Delta H_L &= \Delta H_L^0 + \Delta H_L^{ex} \end{aligned} \qquad (5)$$

where ΔH_G^{ex} and ΔH_L^{ex} are the Gaussian and Lorentzian exchange broadening.

(3) The shape of additionally dipolar broadened components was calculated with expression (3) using the values of width (5).
(4) Inverse Fourier transform was performed to obtain the exchange-broadened and dipolar broadened spectra. These spectra were summed up with definite fractions forming the calculated spectrum. The width of the calculated spectral component was obtained as peak-to-peak distance ΔHpp.
(5) The calculated value of broadening was obtained as the difference between the width of the calculated broadened component and the width of the unbroadened component for low concentration sample.

In the case of the probe A5 the described calculations demonstrate good agreement with the experimental values of broadening only when angle σ is equal to $(90 \pm 10)^\circ$. It means that the vector connecting the two paramagnetic centers is arranged along the director of the liquid crystal. In this case, the expressions (3) and (4) can be appreciably simplified, as dipolar interaction no longer depends on the values of α_L, ψ, and φ. The best description of the experimental broadening is presented in Fig. 4. The corresponding values of parameters are collected in Table 2.

The best description of angular dependence of the broadening for the probe A3 in HOPDOB is also shown in Fig. 4. It is seen that experimental values of broadening are measured with noticeable

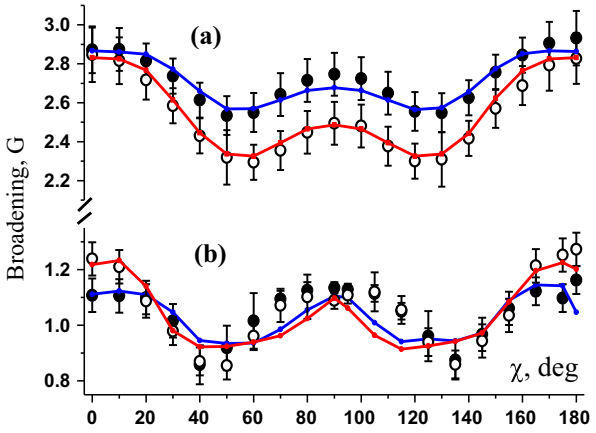

Fig. 4. Experimental (points) and calculated (lines) angular dependences of the concentration broadening for central spectral component of EPR spectra; (a) for probe A5 in SmC HOPDOB (empty points) and SmA HOPDOB (filled points); (b) the same as for probe A3.

Table 2
The characteristics of probe mutual positions determined by the description of the concentration broadening of EPR spectra for radicals A5 and A3 in HOPDOB.

	A5-HOPDOB		A3-HOPDOB	
	SmA	SmC	SmA	SmC
Fraction of probe molecules subjected to magnetic dipolar broadening (molecule in the paired state), α	0.17 ± 0.1	0.30 ± 0.1	0.36 ± 0.1	0.46 ± 0.1
Gaussian exchange broadening, ΔH_G^{ex}	1.5 G	1.75 G	0.55 G	0.55 G
Lorentzian exchange broadening, ΔH_L^{ex}	1.75 G	1.0 G	0.45 G	0.35 G
Distance between nitroxide moieties in pair of probe, R	16.5 ± 0.2 Å	17.0 ± 0.2 Å	16.7 ± 0.2 Å	17.0 ± 0.2 Å
σ	90 ± 10°	90 ± 10°	72.5 ± 1.5°	70 ± 1°
α_L	–	–	0°	20 ± 3°

uncertainty. The errors shown in Fig. 4 is the sum of uncertainties obtained by nonlinear least-square description of spectra for samples with low and high concentrations of probes. It should be noted that experimental errors are contained in the calculated values of broadening as well, because the width of spectra for low concentration of probe was used in the calculation.

Fig. 4 shows that the difference between angular dependences for SmA and SmC mesophases is small. In the case of probe A3 in HOPDOB, this difference is almost negligible relative to experimental uncertainty.

One can see in Fig. 4 that calculated dependences are in accordance with experimental ones. The calculated dependences demonstrated very high sensitivity to the values of parameters. The small deviation from the values presented in Table 2 results in a large change of calculated values of the broadening (see Supplementary Material). Thus, in spite of large experimental uncertainties of determined values of concentration broadening, the structural characteristics of mutual arrangement of radical are determined reliably. The uncertainties of obtained structural parameters are presented in Table 2.

The data presented in Table 2 evidence that the arrangement of pairs of probe molecules connected by dipolar interaction is approximately the same in SmA and SmC mesophases. The most noticeable difference is seen in the fraction of molecules being in the paired state. This value is larger for the SmC phase. The second difference is a somewhat better agreement of experimental and calculated dependences in the case of SmC in comparison with SmA. Both of these differences are obviously the result of poorer alignment of the higher temperature SmA phase. Thus, the SmA phase is characterized by wider and more random distribution of admixture molecules. In addition, the exchange broadening in SmA is somewhat larger than in the SmC phase. This result reflects larger molecular mobility in SmA.

The distance between radicals in pair for probes A5 and A3 were found to be very close. However, the directions of vectors connecting radical centers in pairs of A5 and A3 are different. In the former case, this vector coincides with the liquid crystal director, whereas in the latter case, it is tilted with respect to the director by ~20° ($\sigma \sim 70°$). The probes A5 and A3 differ also by values of exchange broadening. This difference reflects the larger diffusion mobility of A5 caused by relatively smaller molecular size of this radical.

Relative position of the probe molecules in accordance with the data presented in Tables 1 and 2 is shown in Fig. 5. The position of pairs of liquid crystalline molecules is also shown in Fig. 5 for comparison. Coordinates of this pair were determined from the results of X-ray diffraction [45] for crystalline phase of p-hexyloxyphenyl ester of p-octyloxybenzoic acid, which is the closest analog of HOPDOB. The thickness of the smectic layer of HOPDOB has been evaluated earlier as 30.3 Å [46] and 32 Å [47]. The latter value defines the scale of Fig. 5.

The radicals A5 in Fig. 5 are directed by the Y-axis of molecular magnetic frame along the director of liquid crystal (NO bond is perpendicular to director, see angles β and γ in Table 1). The vector connecting radicals A5 in the pair coincides with the director.

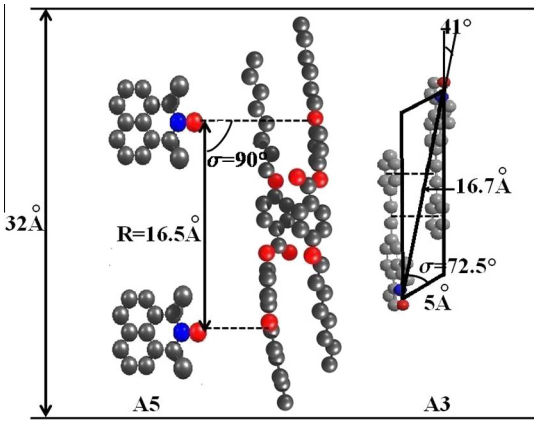

Fig. 5. Relative position of radical probes A3 and A5 subjected to magnetic dipolar interaction, in SmA HOPDOB. The scheme is in accordance with data of Tables 1 and 2 (see text).

Molecular orientation axis of probe A3 is tilted relative to the NO bond by ~41° and, as a whole, coincides with the longest axis of the molecule. The molecules of A3 in the pair are shown in Fig. 5 as parallel, but nitroxide moieties are placed on the opposite ends of the molecules of the pair and one molecule is shifted along the director relative to the second molecule of the pair. These relative positions are in accordance with values R and σ in Table 2.

The mutual position of radicals shown in Fig. 5 leads to some conclusions concerning the nature of intermolecular bonding, which causes the observed ordering. The probe molecule A5 was found to be located in such a manner that aromatic fragments of the radical are close to the aromatic groups of the liquid crystal molecules. Possibly, the radicals are bound with surrounding molecules by π-stacking interactions. At the same time, the NO radical group of pair A5 is at the distance which is equal to the distance between oxygen atoms in the ester bonds of the liquid crystal. Nitroxides are known to form weak bonds with different organic molecules [48]. Obviously, the weak bonding of aromatic and/or nitroxide fragments is responsible for the observed distance between radicals in pairs.

The radicals A3 are able to form the same weak bonds with liquid crystal molecules. Additionally, the relative position of A3 obtained from the analysis of dipolar broadening hints that the pair of A3 radicals is connected by π-stacking interactions between the triple bond of one molecule and the phenylene fragment of the other. The possible weak bonding of radicals in the pair and radicals with liquid crystal molecules is marked in Fig. 5 by dashed lines.

Fig. 5 describes the ordering of the SmA mesophase. The SmC mesophase should be characterized by a nonzero tilt of molecules relative to the layer normal (parameter α_L). The studied systems demonstrate that the direction of radical-to-radical vectors is close to the director of the medium (angle σ is close to 90°). The dipolar

broadening in these conditions becomes low sensitive to the tilt angle α_L. Nevertheless, the calculated angular dependence of the broadening for SmC phase coincides somewhat better with the experimental one if the tilt angle α_L is equal to 20°. This estimation agrees with the value 20–25°, obtained for HOPDOB earlier [49].

4. Conclusions

The presented data demonstrate the angular dependence of magnetic dipole–dipole broadening of EPR spectra for nitroxide spin probe in liquid crystalline media. The analysis of this angular dependence gives the information concerning the molecular structure of liquid crystal as well as localization and mutual positions of probe molecules. The angular dependence appears when nitroxide radicals are able to form specific weak bonds with molecules of liquid crystal and if the radicals occupy definite positions within the structure of liquid crystal. Such situation has been found for liquid crystal HOPDOB. The nitroxide probes in this medium tend to form molecular pairs inside the smectic layers. The geometrical characteristics of the pair have been determined. The smectic 8CB did not demonstrate this phenomenon within the accuracy of experiment.

Acknowledgements

This work was supported by the Russian Foundation for Basic Research, Grant No. 14-03-00323. The authors thank Prof. Rui Tamura (Kyoto University, Japan), Prof. S. Bottle (Queensland University, Australia) and V.K. Cherkasov (Razuvaev Institute of Organometallic Chemistry of RAS, Nizhny Novgorod, Russia) for provision of spin probes.

Appendix A. Supplementary material

Supplementary data associated with this article can be found, in the online version, at http://dx.doi.org/10.1016/j.cplett.2016.05.051.

References

[1] Y.C. Kim, S.H. Lee, J.L. West, E. Gelerinter, Molecular motions and ordering of the interfacial, droplet and binder regions of polymer-dispersed liquid-crystal displays: a paramagnetic-resonance spin-probe study, J. Appl. Phys. 7 (1995) 1914–1922.
[2] C. Serbutoviez, J.G. Kloosterboer, H.M.J. Boots, F.J. Touwslager, Polymerization-induced phase separation. 2. Morphology of polymer-dispersed liquid crystal thin films, Macromolecules 29 (1996) 7690–7698.
[3] C. Serbutoviez, J.G. Kloosterboer, H.M.J. Boots, F.A.M.A. Paulissen, F.J. Touwslager, Polymerization-induced phase separation III. Morphologies and contrast ratios of polymer dispersed liquid crystals, Liq. Cryst. 22 (1997) 145–156.
[4] D. Coates, Polymer-dispersed liquid crystals, J. Mater. Chem. 5 (1995) 2063–2072.
[5] X. Fan, X. Xie, Y. Hatate, Preparation of polymer dispersed liquid crystals using photopolymerization, Chin. J. Polym. Sci. 19 (2001) 311–315.
[6] J.W. Doane, Polymer dispersed liquid crystal displays, in: B. Bahadur (Ed.), Liquid Crystals: Applications and Uses, vol. 1, World Scientific, River Edge, NJ and Singapore, 1990.
[7] J.W. Doane, N.A. Vaz, B.-G. Wu, S. Zumer, Field controlled light scattering from nematic microdroplets, Appl. Phys. Lett. 48 (1986) 269–271.
[8] N.A. Vaz, G.W. Smith, G.P. Montgomery Jr., A light control film composed of liquid crystal droplets dispersed in a UV-curable polymer, Mol. Cryst. Liq. Cryst. 146 (1987) 1–15.
[9] J.L. West, Phase separation of liquid crystals in polymers, Mol. Cryst. Liq. Cryst. 157 (1988) 427–441.
[10] E.E. Burnell, R.Y. Dong, A.C.J. Weber, A. Yethiraj, NMR solutes in nematic and smectic A liquid crystals: the anisotropic intermolecular potential, Magn. Reson. Chem. 52 (2014) 570–580.
[11] A. Yethiraj, A.C.J. Weber, R.Y. Dong, E.E. Burnell, Determination of smectic ordering of probe molecules, J. Phys. Chem. B 111 (2007) 1632–1639.
[12] M.E. Di Pietro, G. Celebre, G. De Luca, H. Zimmermann, G. Cinacchi, Smectic order parameters via liquid crystal NMR spectroscopy: application to a partial bilayer smectic A phase, Eur. Phys. J. E 35 (2012) 112.
[13] J.H. Van Vleck, The dipolar broadening of magnetic resonance lines in crystals, Phys. Rev. 74 (9) (1948) 1168–1183.
[14] W.J.C. Grant, M.W.P. Strandberg, Statistical theory of spin–spin interactions in solids, Phys. Rev. 135 (3A) (1964) 715–726.
[15] C.R. Mao, R.W. Kreilick, Exchange and dipolar interactions in a solid nitroxide radical, Chem. Phys. Lett. 34 (3) (1975) 447–450.
[16] P.W. Anderson, P.R. Weiss, Exchange narrowing in paramagnetic resonance, Rev. Mod. Phys. 25 (1953) 269–276.
[17] P.W. Anderson, A mathematical model for the narrowing of spectral lines by exchange or motion, J. Phys. Soc. Jpn. 9 (1954) 316–339.
[18] W.J.C. Grant, M.W.P. Strandberg, Statistical theory of spin–spin interactions in solids, Phys. Rev. 135 (1964) A715.
[19] N.S. Dalal, A.I. Smirnov, T.I. Smirnova, R.L. Belford, A.R. Katritzky, S.A. Belyakov, Single-crystal multifrequency EPR evidence for a quasi-low-dimensional spin exchange in 3-n-butyl-2,4,6-triphenylverdazyl, J. Phys. Chem. B 101 (1997) 11249–11253.
[20] P. Turek, Spin correlations in organic radical magnets, Mol. Cryst. Liq. Cryst. 233 (1) (1993) 191–207.
[21] A.Kh. Vorobiev, N.A. Chumakova, D.A. Pomogailo, Y. Uchida, K. Suzuki, Y. Noda, R. Tamura, Determination of structural characteristics of all-organic radical liquid crystals based on analysis of the dipole–dipole broadened EPR spectra, J. Phys. Chem. B 118 (2014) 1932–1942.
[22] D.S. Hulme, E.P. Raynes, K.J. Harrison, Eutectic mixtures of nematic 4′-substituted 4-cyanobiphenyls, J. Chem. Soc., Chem. Commun. 98–99 (1974).
[23] V. Vill, LiqCryst 5.0 – Database of Liquid Crystalline Compounds, LCI Publisher, Hamburg, 2010. <liqcryst.lci-publisher.com>.
[24] S. Petrov, P. Simova, The smetic polymorphism and the phase transitions in the liquid crystal 4, n-hexyloxyphenyl-4, n′-decyloxybenzoate, Cryst. Res. Technol. 21 (1986) 959–965.
[25] N. Ikuma, R. Tamura, S. Shimono, N. Kawame, O. Tamada, N. Sakai, J. Yamauchi, Y. Yamamoto, Magnetic properties of all-organic liquid crystals containing a chiral five-membered cyclic nitroxide unit within the rigid core, Angew. Chem. Int. Ed. 43 (2004) 3677–3682.
[26] N. Ikuma, R. Tamura, S. Shimono, Y. Uchida, K. Masaki, Y. Yamauchi, Y. Aoki, H. Nohira, Ferroelectric properties of paramagnetic, all-organic, chiral nitroxyl radical liquid crystals, Adv. Mater. 18 (2006) 477–480.
[27] J.P. Blinco, J.C. McMurtrie, S.E. Bottle, The first example of an azaphenalene profluorescent nitroxide, Eur. J. Org. Chem. 28 (2007) 4638–4641.
[28] D.J. Keddie, K.E. Fairfull-Smith, S.E. Bottle, The palladium-catalysed copper-free Sonogashira coupling of isoindoline nitroxides: a convenient route to robust profluorescent carbon–carbon frameworks, Org. Biomol. Chem. 6 (17) (2008) 3135–3143.
[29] A. Nayeem, S.B. Rananavare, V.S.S. Sastry, J.H. Freed, Heisenberg spin exchange and molecular diffusion in liquid crystals, J. Chem. Phys. 91 (1989) 6887–6905.
[30] N.A. Chumakova, V.I. Pergushov, A.Kh. Vorobiev, A.I. Kokorin, Rotational and translational mobility of nitroxide spin probes in ionic liquids and molecular solvents, Appl. Magn. Reson. 39 (2010) 409–421.
[31] B.-K. Shin, An analytical method for the deconvolution of Voigtian profiles, Appl. Magn. Reson. 47 (2016) 429–452.
[32] S.M. Abrarov, B.M. Quineb, R.K. Jagpal, A simple interpolating algorithm for the rapid and accurate calculation of the Voigt function, J. Quant. Spectrosc. Radiat. Transfer 110 (6) (2009) 376–383.
[33] M.H. Mendenhall, Fast computation of Voigt functions via Fourier transforms, J. Quant. Spectrosc. Radiat. Transfer 105 (2007) 519–524.
[34] V. Parthasarathi, S. Ganapathy, C.A. McDowell, The evaluation and characterization of Voigt lineshape, J. Mol. Struct. 64 (1980) 29–38.
[35] A.Kh. Vorobiev, N.A. Chumakova, Simulation of rigid-limit and slow-motion EPR spectra for extraction of quantitative dynamic and orientational information, in: A.I. Kokorin (Ed.), Nitroxides – Theory, Experiment and Applications, INTECH, Rijeka, 2012.
[36] S.N. Dobryakov, Ya.S. Lebedev, Analysis of spectral lines whose profile is described by a composition of Gaussian and Lorentz profiles, Dokl. Acad. Nauka SSSR 182 (1968) 68–70.
[37] G.M. Jidomirov, Ya.S. Lebedev, S.N. Dobryakov, N.Ya. Shteinshneider, A.K. Chirkov, V.A. Gubanov, Interpretation of Complex ESR Spectra, Nauka, Moscow, 1975, p. 216 (in Russian).
[38] J.E. Dennis, D.M. Gay, R.E. Welseh, An adaptive nonlinear least-squares algorithm, ACM Trans. Math. Softw. 7 (3) (1981) 348–383.
[39] D.E. Budil, S. Lee, S. Saxena, J.H. Freed, Nonlinear-least-squares analysis of slow-motion EPR spectra in one and two dimensions using a modified Levenberg–Marquardt algorithm, J. Magn. Reson. Ser. A 120 (1996) 155–189.
[40] N.A. Chumakova, D.A. Pomogailo, T.S. Yankova, A.Kh. Vorobiev, The novel stable nitroxide radicals as perspective spin probes for study of orientation order of liquid crystals and polymers, Mol. Cryst. Liq. Cryst. 540 (2011) 196–204.
[41] T.S. Yankova, N.A. Chumakova, D.A. Pomogailo, A.Kh. Vorobiev, Spin probe orientation distribution functions in aligned nematic liquid crystal, Magn. Reson. Solids 13 (2011) 10–13.
[42] T.S. Yankova, N.A. Chumakova, D.A. Pomogailo, A.Kh. Vorobiev, Orientational order of guest molecules in aligned liquid crystal as measured by EPR and UV–vis techniques, Liq. Cryst. 40 (2013) 1135–1145.
[43] N.A. Chumakova, T.S. Yankova, K.E. Fairfull-Smith, S.E. Bottle, A.Kh. Vorobiev, Molecular orientational order of nitroxide radicals in liquid crystalline media, J. Phys. Chem. B 118 (2014) 5589–5599.
[44] J.P. Barnes, J.H. Freed, Dynamics and ordering in mixed model membranes of dimyristoylphosphatidylcholine and dimyristoylphosphatidylserine: a 250-GHz electron spin resonance study using cholestane, Biophys. J. 75 (1998) 2532–2546.

[45] M.A. Gunina, N.S. Kucherepa, S.M. Pestov, L.G. Kuz'mina, Crystal and molecular structure of n-hexyloxyphenyl n-octyloxybenzoate, Crystallogr. Rep. 57 (2012) 524–527.
[46] V.K. Dolganov, E.I. Demikhov, R. Fouret, C. Gors, Free-standing films above the bulk smectic–nematic–isotropic transitions, Phys. Lett. A 220 (1996) 242–246.
[47] H. Schüring, R. Stannarius, Surfaces and interfaces of free-standing smectic films, in: R. Haberlandt, D. Michel, A. Pöppl, R. Stannarius (Eds.), Molecules in Interaction with Surfaces and Interfaces, Springer, Heidelberg, 2014.
[48] A.L. Buchachenko, Complexes of Radicals and Molecular Oxygen with Organic Molecules, Nauka, Moscow, 1984, p. 157 (in Russian).
[49] M.A. Glaser, Atomistic simulation and modeling of smectic liquid crystals, in: P. Pasini, C. Zannoni (Eds.), Advances in the Computer Simulations of Liquid Crystals, NATO Science Series, Erice, 2000.